XLIII CILAMCE
21–25, November, 2022
FOZ DO IGUAÇU – PR – BRAZIL

Micromechanical Approach to the Effective Poroelastic Behavior of Jointed Rock Masses under One-Dimensional Consolidation and Finite Element Implementation

Augusto B. Borges[1], Samir Maghous[1]

[1]*PPGEC/CEMACOM, Federal University of Rio Grande do Sul*
Av. Osvaldo Aranha, 99, 3rd floor - CEMACOM, 900.35-190, Rio Grande do Sul, Brazil
augustobopsinborges@gmail.com, samir.maghous@ufrgs.br

Abstract. A micromechanics-based formulation of the macroscopic behavior of saturated jointed rocks regarded as homogenized anisotropic poroelastic media is presented. At the material level, the rock matrix forming the skeleton phase of the porous medium is assumed to be linear elastic, whereas the crosscutting joints stand for the porous space and are viewed as planar interfaces endowed with a specific generalized poroelastic behavior. The effective anisotropic poroelastic properties, including the homogenized drained elastic stiffness tensor $\mathbb{C}$, Biot tensor $\underline{\underline{B}}$, Biot modulus $\mathcal{M}$, as well as the permeability tensor $\underline{\underline{K}}$ of the jointed medium are derived. At the structure level, the consolidation problem of a jointed rock layer is addressed in a one-dimensional setting with anisotropic flow conditions introduced by joints orientations. For verification purpose, the analytical predictions derived from the analysis are compared with finite element solutions implementing the effective constitutive state equations, thus emphasizing that the analytical predictions can be viewed as reference solutions.

Keywords: jointed rock, microporoelasticity, finite element method, one-dimensional consolidation

1 Introduction

Understanding of the hydromechanical behavior of fractured rock media is a key aspect for safety and stability evaluation of large engineering rock works such as rock slopes, waste disposal repositories, dam foundations, underground excavations, as well as assessment of the transport of fluid or contaminants, exploitation wells for extraction of underground water and hydrocarbons, foundations of geothermal, thermal, hydroelectric and nuclear power plants, and so on. The increasingly common land subsidence effects, triggered by extraction of large amounts of water and/or oil from natural resources reservoirs (Jones and Addis [1], Gambolati et al. [2]), and the consequent effect in recovery capacity of such natural resources, as well as social connected problems, demonstrate the relevance of coupled hydromechanical modeling for jointed rock media. When rock matrix permeability is low, the fractures present in the rock mass, usually referred to as joints, form connected networks that serve as preferential channels for fluid flow, as well as surfaces where the mechanical properties of the rock matrix degrade. Therefore, design analyses involving saturated rock masses, from a geomechanical point of view, need to incorporate an accurate and comprehensive modeling for the joints through a poromechanical coupling.

Over the last few decades, efforts have been made to study and characterize the behavior of jointed rock masses, both via semi-empirical approaches based on rock mass classification systems and coupling strength, deformation, and permeability of jointed rock masses (Deere and Miller [3], Hoek and Brown [4]). In general, most representative works concerning hydromechanical coupling in rock joints are focused on the connection between normal or shear loading/unloading effect on the joint permeability (Witherspoon et al. [5], Tsang and Witherspoon [6], Bandis et al. [7], Barton et al. [8], Oda [9]). In such approaches, the effect of fluid pressure filling the joints is usually neglected or considered indirectly by variations in joint hydraulic opening as a function of stress level. Poromechanical models for joints behavior are still relatively rare in the literature (Ng and Small [10], Bart et al. [11]).

Since rock joint and rock matrix behavior are determined and modeled separately, the assessment of representative constitutive models for each individual behavior of rock joints and rock matrix is usually not a simple task. The numerical modeling and implementation for analysis and evaluation of structures on jointed rock is traditionally performed explicitly, introducing individual joints in a impermeable/permeable, deformable/rigid rock matrix, and enabling consideration of complex fracturing patterns (Goodman [12], Cundall [13]). However,

the denser the fracture network, or when there is a need for full-scale modeling of rock masses and natural reservoirs, such an explicit approach may become computationally unfeasible by current computational standards. Implicit homogenization approaches, on the other hand, were conceived as an alternative to discrete explicit approaches, based on the idea that a heterogeneous medium, such as a jointed rock mass, can be treated at the macroscopic scale as a continuous and homogeneous medium (Zaoui [14]). The well-known Hoek and Brown [15] empirical strength criterion for jointed mass, for instance, takes advantage of this idea in a purely macroscopic phenomenological approach.

Aiming to derive the jointed rock mass effective poroelastic behavior from those of the rock matrix and rock joints, Maghous et al. [16] proposed a micromechanical approach to the poroelastic behavior of jointed rocks by assuming rock joints as forming the porous space of the rock mass, with their behavior governed by a poroelastic interface constitutive law analogous to the classical poroelastic state equations of an ordinary porous medium (Bart et al. [11]). Starting from the local behavior of the rock matrix as an elastic solid and joints modeled as generalized porous media, the upscaling process allows the effect of fluid pressure in the interstitial rock joint space to be taken into account in the effective macroscopic behavior, as well as rock joint pore volume changes. The classical effective poroelastic state equations are derived with effective poroelastic parameters determined from rock matrix elastic parameters, rock joint stiffness, generalized rock joint Biot coefficient and Biot modulus, spatial distribution and orientation.

In modeling jointed rock masses as porous media, the classic consolidation problem needs to be addressed. As jointed rock masses are generally anisotropic, both mechanically and hydraulically, it is expected that the solution to the consolidation problem in fractured media takes this aspect into account. Analytical and semi-analytical solutions were presented in the literature for transversely isotropic soils with respect to the hydraulic behavior, and isotropic mechanical behavior (Booker and Randolph [17], Ai and Wu [18], Rani et al. [19]), as well as some numerical approaches to the problem in jointed rocks (Sasaki and Morikawa [20]).

In that context, this article aims to present analytical solution for particular cases of mechanically isotropic and hydraulically anisotropic jointed rock masses under one-dimensional consolidation. Jointed rock masses crosscut by one and two joint sets, as well as for randomly oriented joint sets are considered. The latter, however, results in a fully isotropic poroelastic medium, and serves as a verification problem for an *ad hoc* numerical finite element implementation.

2 Effective Poroelastic Properties and Permeability of Jointed Rocks

Consider a rock mass crosscut by sets of long joints. Based on micromechanical principles (Zaoui [14]) a representative elementary volume (REV) can be defined for the jointed rock mass provided conditions for separation of scales holds. In other words, the characteristic size of the joints, identified as the average spacing between joints of a given set ω (d) must be much smaller than the characteristic size of the REV (ℓ). Further, the characteristic size of the REV must be much smaller than the characteristic dimension of the macroscopic structure under consideration $(\mathcal{L})$. Summing up, we must have $d \ll \ell \ll \mathcal{L}$.

In this sense, considering joints as the connected porous space of a jointed rock mass and assuming a generalized poroelastic behavior for the joints, Maghous et al. [16] presented a micromechanical formulation for the effective poroelastic properties of rock masses, crosscut by planar long joints, from those of the individual constituents (rock matrix stiffness $\mathbb{C}^s$ and compliance $\mathbb{S}^s$ fourth order tensors, normal $\mathtt{k}_n$ and tangential $\mathtt{k}_t$ joint stiffness – assembled in a joint stiffness second order tensor $\underline{\underline{\mathtt{k}}}$, joint Biot modulus m and joint Biot coefficient α). Joints distribution is defined by spatial orientation, defined by its normal unit vector $\underline{\mathtt{n}}$, and by joint average spacing d. Although it is a well-known and used result Goodman [21], the Authors rigorously derived the localization problem giving the effective elastic compliance tensor $\mathbb{S}$ as the sum of rock matrix $(\mathbb{S}^s)$ and joint sets $(\mathbb{S}^{\omega_j})$ contributions. Other effective poroelastic parameters (Biot tensor $\underline{\underline{B}}$ and Biot modulus $\mathcal{M}$) are readily determined from characteristics of the rock matrix, joints, as well as from effective drained elastic moduli tensors. It is worth to note that, when scale separation is ensured, $\mathbb{C} \approx \mathbb{S}^{-1}$.

Based on the same arguments ensuring validity of the micromechanical reasoning, Borges and Maghous [22] presented the effective intrinsic permeability or, equivalently, the permeability tensor $\underline{\underline{K}}$ for rock masses cut by long joints, considering permeable or impervious rock matrix crosscut by long joints.

Both micromechanical formulations allow consideration of either discrete or randomly oriented joint sets.

3 One-dimensional consolidation problem of a jointed rock layer

Consider an infinite half-space of jointed rock mass with thickness h resting on a rigid impervious base $(x_3 = h)$ and subjected to an uniform surface load increment ($\Delta\sigma_{33} = -q$ at $x_3 = 0$) as shown in Fig. 1.

When such a jointed rock layer, modeled as homogeneous porous material, is subjected to an additional load with respect to gravity, the saturating fluid undergoes an increment of fluid pressure (pore pressure) Δp. Subsequently, pore pressure continuously vanish due to fluid diffusion towards the drained surface, while the mechanical load is progressively transferred to solid skeleton, thus resulting in upper surface settlement.

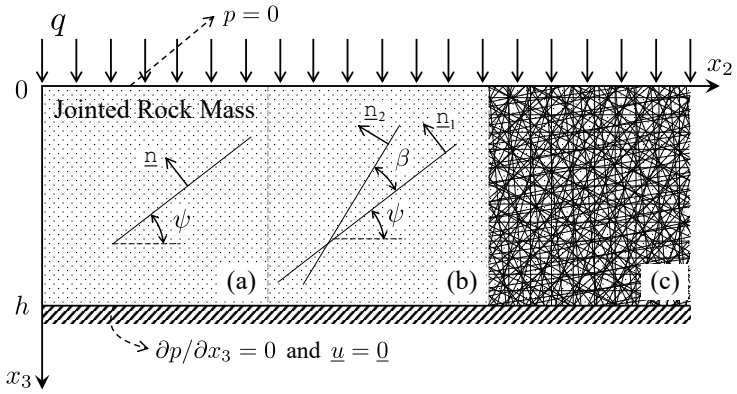

Figure 1. Consolidation of a jointed rock mass considering (a) one joint set (b) two joint sets, and (c) randomly oriented joint sets – isotropic joint distribution.

For the sake of simplicity, analytical and numerical results for the three cases of one-dimensional consolidation of a jointed rock mass with isotropic poroelastic and anisotropic hydraulic behavior are presented (cases of Fig. 1a, b and c). Under one-dimensional consolidation conditions, pore pressure p and displacement $\underline{u}$ are functions of depth only ($p = p(x_3)$ and $\underline{u} = u(x_3)\underline{e}_3$). Consequently, the second order strain tensor, volumetric strain, and pore pressure gradient are, respectively, given by $\underline{\underline{\varepsilon}} = \partial u/\partial x_3 \underline{e}_3 \otimes \underline{e}_3$, $\varepsilon_v = \mathrm{tr}\ \underline{\underline{\varepsilon}} = \partial u/\partial x_3$, and $\nabla p = \partial p/\partial x_3 \underline{e}_3$.

Assuming small perturbations hypothesis, the macroscopic poroelastic state equations governing the skeleton behavior reads:

$$\begin{cases} \Delta\underline{\underline{\sigma}} = \mathbb{C} : \underline{\underline{\varepsilon}} - \underline{\underline{B}}\Delta p & \text{(a)} \\ \Delta\phi = \underline{\underline{B}} : \underline{\underline{\varepsilon}} + \Delta p/\mathcal{M} & \text{(b)} \end{cases} \tag{1}$$

where $\underline{\underline{\sigma}}$ and $\underline{\underline{\varepsilon}}$ are, respectively, the macroscopic stress and strain tensors, and ϕ is the Lagrangian porosity.

The fluid flow is macroscopically governed by Darcy's Law:

$$\underline{\mathcal{Q}} = -\underline{\underline{K}} \cdot \nabla\left(\Delta p\right), \tag{2}$$

where $\underline{\mathcal{Q}}$ is the macroscopic filtration or specific discharge vector. The fluid continuity equation reads:

$$\frac{\partial \phi}{\partial t} + \mathrm{div}\ \underline{\mathcal{Q}} = 0. \tag{3}$$

Substituting Darcy's Law (eq. (2)) and the second poroelastic state equation (eq. (1b)) in the fluid continuity equation (eq. (3)), the coupled equation governing the fluid diffusion through a porous medium is obtained as:

$$\underline{\underline{B}} : \frac{\partial \underline{\underline{\varepsilon}}}{\partial t} + \frac{1}{\mathcal{M}}\frac{\partial p}{\partial t} = \underline{\underline{K}} : \nabla\left[\nabla\left(\Delta p\right)\right]. \tag{4}$$

The one-dimensional consolidation problem of a fully isotropic porous medium ($\mathbb{C} = \lambda \underline{\underline{1}} \otimes \underline{\underline{1}} + 2\mu\mathbb{I}$, $\underline{\underline{B}} = b\underline{\underline{1}}$, and $\underline{\underline{K}} = \mathcal{K}\underline{\underline{1}}$), considering geometry and boundary conditions as expressed in Fig. 1, is a well-known textbook problem in poromechanics (Coussy [23]). The solution for fully isotropic case, in terms of pore pressure excess, can be expressed as:

$$\Delta p(x_3, t) = \frac{4b\mathcal{M}q}{\lambda + 2\mu + b^2\mathcal{M}} \sum_{n=0}^{\infty} \frac{1}{(2n+1)\pi} \sin\left[\frac{(2n+1)\pi}{2h} x_3\right] \exp\left[-\frac{(2n+1)^2\pi^2 c_f}{4h^2} t\right]. \tag{5}$$

where $c_f = \mathcal{K}\mathcal{M}(\lambda + 2\mu)/(\lambda + 2\mu + b^2\mathcal{M})$ is known as the diffusion/consolidation coefficient.

After the instantaneous load increment application $\Delta\sigma_{33} = -q$ at the upper surface ($x_3 = 0$), equilibrium in the vertical direction requires $\Delta\sigma_{33}(x_3) = -q$ ($\forall x_3$). So, considering the first poroelastic state equation (eq. (1a)), the equilibrium condition ($\mathrm{div}\ \Delta\underline{\underline{\sigma}} = \underline{0}$), and the fact that displacement $\underline{u}$ is purely vertical, it can be shown that:

$$\frac{\partial u}{\partial x_3}(x_3, t) = \frac{q}{\lambda + 2\mu}\left(\frac{b}{q}\Delta p(x_3, t) - 1\right). \tag{6}$$

Integrating eq. (6) over depth and considering that $u(h,t) = 0$ (Fig. 1) provides:

$$u(0,t) = s(t) = s_\infty + (s_0 - s_\infty) \sum_{n=0}^{\infty} \frac{8}{(2n+1)^2 \pi^2} \exp\left[-\frac{(2n+1)^2 \pi^2 c_f}{4h^2} t \right], \tag{7}$$

where s_0 and s_∞ are, respectively, the instantaneous (undrained) and long-term (drained) settlements, given by:

$$s_0 = \frac{qh}{\lambda + 2\mu + b^2 \mathcal{M}}; \quad s_\infty = \frac{qh}{\lambda + 2\mu}, \tag{8}$$

and $s(t)$ is the settlement of the upper surface.

As the pore pressure gradient is a function only of x_3, it can be seen from eq. (4) that, even in the fully isotropic case, the only component of the permeability tensor left from right-hand size operation is K_{33}. In other words, in the one-dimensional consolidation problem defined in Fig. 1, the only permeability tensor component involved is K_{33}.

It can be shown that, referring to cases (a) and (b) in Fig. 1, when anisotropic hydraulic behavior and identical joint sets characteristics are assumed, consolidation will be one-dimensional only if *Case (a)* $\psi = \pi/2$ ('vertical' joint set); *Case (b)* $\beta = \pi - 2\psi$ (joint sets symmetrically oriented with respect to the 'vertical'). A particular feature referring to *Case (b)* is that, when perpendicular joint sets are considered ($\beta = \pi/2$), the permeability tensor turns out to be independent of ψ. *Case (c)* results in isotropic hydraulic behavior, since joint sets are randomly oriented, and therefore, isotropic distributed in space.

Complying with the stated conditions for one-dimensional consolidation in cases (a) and (b), the solution for all three cases considered in Fig. 1, as well as for the particular *Case (b)* when joint sets are perpendicular to each other, have the same form of that given in eq. (5). The only difference is the use of the respective K_{33} component of $\underline{\underline{K}}$, since $\underline{\underline{K}}$ is no longer isotropic (except in *Case (c)*).

Based on Borges and Maghous [22], K_{33} permeability component calculated for particular case (a) and (b) stated above reads:

$$K_{33} = f \left[k_t^{(1)} \sin^2 \psi + k_t^{(2)} \sin^2 (\psi + \beta) \right], \tag{9}$$

where $k_t^{(1)}$ and $k_t^{(2)}$ stand, respectively, for the tangential joint permeability of the joint sets 1 and 2 (when it's present), and f stands for the volume fraction of individual joint sets. For case (c), considering an unique tangential permeability k_t for randomly oriented joint sets, it reads:

$$K_{33} = \mathcal{K} = \frac{2}{3} f k_t. \tag{10}$$

These analytical results can be used as a benchmark for verification of numerical implementations of two- and three-dimensional codes in coupled poroelasticity with anisotropic hydraulic behavior. It is noted that short- (undrained) and long-term (drained) solutions do not depend on joint permeability. The only difference between cases is the time needed for reaching long-term regime, which is affected by K_{33} value. Defining the characteristic consolidation time as $\tau = h^2/c_f$, it can be readily seen that the only changing parameter on eq. (5) is the relevant permeability coefficient for each case.

4 Numerical Simulations

The micromechanical formulations for the hydromechanical behavior of jointed rock (Maghous et al. [16], Borges and Maghous [22]) were recently implemented in a version of a three-dimensional finite element numerical code originally developed in Brüch [24] for isotropic effective behavior.

In order to verify the numerical implementation and demonstrate the analytical solution presented in section 3, a number of one-dimensional numerical simulations of mechanically isotropic jointed rock medium with anisotropic hydraulic behavior were performed. The finite element procedure used in assessing the evolution of the jointed rock mass, adapted to anisotropic poroelasticity, is found in Bernaud et al. [25]. Hexahedral 20-node elements are used for geometry discretization with piece-wise quadratic polynomial function for displacement approximation, superposed with 8-node elements with linear function for pore pressure approximation. The resulting global equation system is expressed as:

$$\begin{bmatrix} [\mathbf{K_{UU}}] & [\mathbf{K_{UP}}] \\ [\mathbf{K_{PU}}] & [\mathbf{K_{PP}}] \end{bmatrix} \begin{Bmatrix} \{\mathbf{U}\} \\ \{\mathbf{P}\} \end{Bmatrix} = \begin{Bmatrix} \{\mathbf{F_U}\} \\ \{\mathbf{F_P}\} \end{Bmatrix} \tag{11}$$

where $[\mathbf{K_{IJ}}]$ are the global stiffness sub-matrices, $\{\mathbf{F_I}\}$ the global force sub-vectors, while $\{\mathbf{U}\}$ and $\{\mathbf{P}\}$ are, respectively, the nodal displacement and pore pressure global vectors.

In one-dimensional consolidation, a single column of elements is enough to simulate the process as an infinite horizontal layer. Therefore, the numerical model constructed to simulate the cases considered in Fig. 1 consists in a column of jointed rock $h = 6$ km high, with a square base parallel to (x, y) plane and horizontal side of $h/60$. Vertically, the finite element mesh divides the column in 60 equal parts (60 finite elements in total), forming a regular mesh with cubic elements of $h/60$ side. All vertical boundaries are impervious and horizontally restrained ($\underline{u}\cdot\underline{e}_i = \underline{\mathcal{Q}}\cdot\underline{e}_i = 0\,(i = x, y)$), while at the bottom no fluid flow or displacement is allowed ($\underline{u}\cdot\underline{e}_z = \underline{\mathcal{Q}}\cdot\underline{e}_z = 0$). An uniformly distributed loading $q = 10$ MPa is instantaneous applied at the upper surface of the model maintaining drainage ($p = 0$).

Numerical simulations were performed considering the effective poromechanical medium as isotropic, with $\lambda = 4.0$ GPa, $\mu = 4.0$ GPa ($E = 10$ GPa and $\nu = 0.25$), $b = 0.75$, and $\mathcal{M} = 20$ GPa. The settlement of the upper surface and excess pore pressure dissipation during the consolidation process is presented in Fig. 2 for the three cases considered. The instantaneous and long-term settlements, calculated by eq. (7), results $s_0/h = 4.30 \times 10^{-4}$ and $s_\infty/h = 8.33 \times 10^{-4}$. In Fig. 2, continuous lines refer to analytical solution, whereas markers refer to finite element predictions.

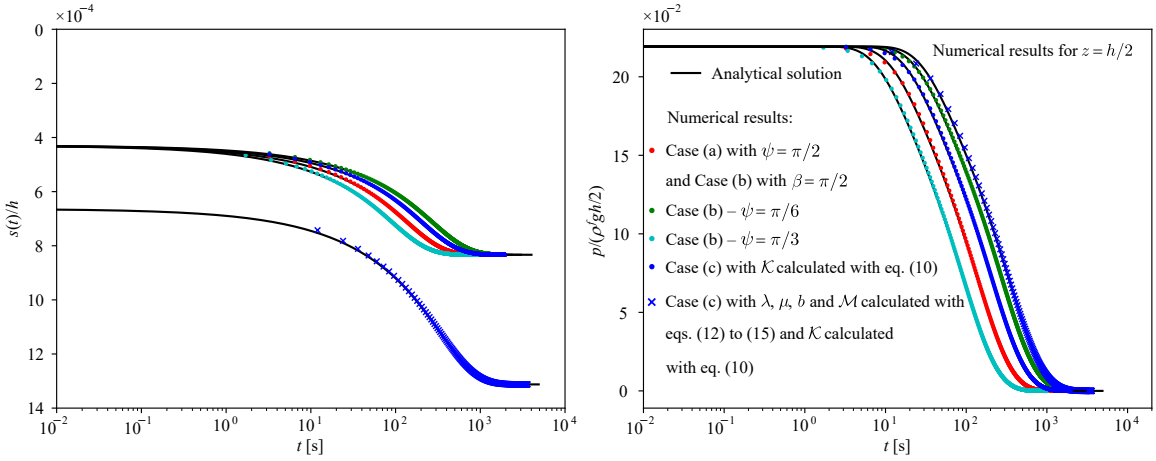

Figure 2. Analytical solution and numerical simulations results for settlement (a) and excess pore pressure dissipation at $z = h/2$ (b) during consolidation process of a jointed rock mass layer with $h = 6$ km high and superficial water table.

In addition, in order to verify the numeric implemented formulation for the effective properties of jointed rocks with randomly oriented joint sets in poroelasticity, *Case (c)* has been also numerically simulated with effective poroelastic parameters calculated using the micromechanical formulation presented in Maghous et al. [16]. In the numerical implementation, user inputs rock matrix elastic parameters (E^s, ν^s), joint stiffness k_n and k_t, average spacing d, joint Biot coefficient α, joint Biot modulus m, and joints volume fraction f. The effective poroelastic parameters (λ, μ, b, and $\mathcal{M}$) are automatically calculated during processing. A randomly oriented joint distribution results in a isotropic effective hydromechanical behavior, with effective poroelastic parameters calculated as:

$$\lambda = 3\mathrm{k}_n d\frac{2\mu^s\left(3\lambda^s + 2\mu^s\right)\left(\mathrm{k}_n - \mathrm{k}_t\right) + 15\lambda^s\mathrm{k}_n\mathrm{k}_t d}{\left(2\mu^s\left(3\mathrm{k}_n + 2\mathrm{k}_t\right) + 15\mathrm{k}_n\mathrm{k}_t d\right)\left(3\lambda^s + 2\mu^s + 3\mathrm{k}_n d\right)}, \tag{12}$$

$$\mu = \mu^s\frac{15\mathrm{k}_n\mathrm{k}_t d}{2\mu^s\left(3\mathrm{k}_n + 2\mathrm{k}_t\right) + 15\mathrm{k}_n\mathrm{k}_t d}, \tag{13}$$

$$b = \alpha\frac{3\lambda^s + 2\mu^s}{3\lambda^s + 2\mu^s + 3\mathrm{k}_n d}, \tag{14}$$

$$\mathcal{M} = \left(\frac{1}{m\,d} + \frac{3\alpha^2}{3\lambda^s + 2\mu^s + 3\mathrm{k}_n d}\right)^{-1}, \tag{15}$$

and permeability coefficient given in eq. (10).

In this configuration that falls within *Case (c)*, the rock matrix elastic parameters were assumed as $\lambda^s = 10.0$ GPa, $\mu^s = 10.0$ GPa ($E^s = 25$ GPa and $\nu^s = 0.25$), while joints parameters as $\alpha = 1.0$, and $m = 30$ GPa, $\mathrm{k}_n = 5.0$ GPa/m, $\mathrm{k}_t = 2.0$ GPa/m, and $d = 1.0$ m. The effective poroelastic parameters calculated by eqs. (12) to (15) results in $\lambda = 1.96$ GPa, $\mu = 2.83$ GPa ($E = 6.82$ GPa and $\nu = 0.20$), $b = 0.77$, and $\mathcal{M} = 12.58$ GPa.

For this case, analytical solution and the numerical simulations results are also shown in Fig. 2. The respective instantaneous and long-term settlement calculated are $s_0/h = 6.63 \times 10^{-4}$ and $s_\infty/h = 1.31 \times 10^{-3}$.

For all cases, with respect to the relevant hydraulic parameters, $e = 5$ mm, and $d = 1.0$ m were adopted. Also, the rock matrix unit weight was set as $\rho^s = 3{,}000$ kg/m^3 and fluid unit weight as $\rho^f = 1{,}000$ kg/m^3. The joint tangential permeability for all joint sets was taken as $k_t = 2.08{\times}10^{-3}$ m^2/(Pa·s). As the gravitational forces are constant and no external horizontal forces of any kind are considered, the uniform superficial load increment q is the only involved in the consolidation process.

Regarding the analytical solution presented in Fig. 2, as expected, when the mechanical effects due to the presence of joints are not taken into account, the same instantaneous (undrained) and long-term (drained) response is obtained in all cases (a), (b) and (c). The only difference is the transient response, function of the permeability coefficient K_{33} for each case considered. Regarding the numerical results, a very good agreement between them and the analytical solution were obtained using a fairly coarse finite element mesh, even for early times.

The degradation caused by the presence of the joints on the overall hydromechanical mechanical behavior of a consolidating jointed rock mass can be verified comparing the overall response presented for case (c) and its variation accounting for joints degradation in Fig. 2. It can be seen that degradation of the poromechanical properties is reflected both in the computed displacements and time required to reach the long-term regime.

5 Conclusions

Analytical solution of one-dimensional consolidation problem for particular cases of rock masses crosscut by long planar joints were given, taking the jointed rock mass under consolidation as mechanically isotropic and hydraulically anisotropic. Three simple cases were considered taking jointed rock masses crosscut by one and two joint sets, as well as by randomly oriented joint sets. The conditions for one-dimensional consolidation were stated, and the difference between the solution for the considered cases and that of a fully isotropic medium outlined. This analytical solution can serve as a benchmark to verification of numerical implementation of codes in anisotropic linear poroelasticity.

The hydraulic behavior of the effective jointed medium was determined through a micromechanical approach, considering impermeable rock matrix and joints tangential permeability. Classically, the joints tangential permeability may be estimated based on the plane Poiseuille flow (cubic-law). Explicit analytical expressions were also given for the effective poroelastic parameters of a jointed rock with randomly oriented joint sets based on the micromechanical formulation of Maghous et al. [16].

For the one-dimensional consolidation problem of jointed rock masses, it has been identified that the relevant permeability coefficient is the only changing variable considering the solution for fully isotropic case. Disregarding the poromechanical degradation due to the joints, the difference between the results occurs only in the time required for the consolidation process to finish. Considering poromechanical degradation due to joints, however, its relevance for the complete characterization of the poroelastic response of a rock mass in consolidation is highlighted. Practical application of these results would be, for instance, to problems involving foundation settlement under loads, time-dependent behavior of embankments, dams, wells, as well as underground excavations, underground military facilities, etc.

In order to perform a verification of an *in house* finite element implementation in anisotropic poroelasticity, several numerical simulations were performed and the results plotted against the given analytical solution for the one-dimensional consolidation problem of jointed rocks. The numerical results are in line with the given analytical solution, ensuring and verifying the correct numerical implementation of the finite element formulation, both for anisotropic flow and for the implemented poroelastic and hydraulic behavior of randomly oriented joint sets. The analytical solution of the consolidation problem for a fully anisotropic jointed rock mass, as well as related numerical examples, will be the subject of a forthcoming article.

Acknowledgements. The authors are greateful for the financial support of the Brazilian National Council for Scientific and Technological Development (CNPq), and for the Federal University of Rio Grande do Sul.

Authorship statement. The authors hereby confirm that they are the sole liable persons responsible for the authorship of this work, and that all material that has been herein included as part of the present paper is either the property (and authorship) of the authors, or has the permission of the owners to be included here.

References

[1] Jones, M. E., L. M. J. & Addis, M. A., 1987. Reservoir compaction and surface subsidence due to hydrocarbon extraction.
[2] Gambolati, G., Ferronato, M., & Teatini, P., 2006. Reservoir compaction and land subsidence. *Revue Européenne de Génie Civil*, vol. 10, n. 6-7, pp. 731–762.
[3] Deere, D. U. & Miller, R. P., 1966. Engineering Classification and Index Properties for Intact Rock. Technical report, Air Force Weapons Laboratory, Kirtland.
[4] Hoek, E. & Brown, E. T., 2019. The Hoek–Brown failure criterion and GSI – 2018 edition. *Journal of Rock Mechanics and Geotechnical Engineering*, vol. 11, n. 3, pp. 445–463.
[5] Witherspoon, P. A., Wang, J. S. Y., Iwai, K., & Gale, J. E., 1980. Validity of Cubic Law for fluid flow in a deformable rock fracture. *Water Resources Research*, vol. 16, n. 6, pp. 1016–1024.
[6] Tsang, Y. W. & Witherspoon, P. A., 1981. Hydromechanical behavior of a deformable rock fracture subject to normal stress. *Journal of Geophysical Research*, vol. 86, n. B10, pp. 9287–9298.
[7] Bandis, S. C., Lumsden, A. C., & Barton, N. R., 1983. Fundamentals of rock joint deformation. *International Journal of Rock Mechanics and Mining Sciences*, vol. 20, n. 6, pp. 249–268.
[8] Barton, N. R., Bandis, S. C., & Bakhtar, K., 1986. Strength, Deformation and Conductivity Coupling of Rock Joints. *Publikasjon - Norges Geotekniske Institutt*, vol. 22, n. 162, pp. 121–140.
[9] Oda, M., 1986. An equivalent continuum model for coupled stress and fluid flow analysis in jointed rock masses. *Water Resources Research*, vol. 22, n. 13, pp. 1845–1856.
[10] Ng, K. L. A. & Small, J. C., 1997. Behavior of joints and interfaces subjected to water pressure. *Computers and Geotechnics*, vol. 20, n. 1, pp. 71–93.
[11] Bart, M., Shao, J. F., Lydzba, D., & Haji-Sotoudeh, M., 2004. Coupled hydromechanical modeling of rock fractures under normal stress. *Canadian Geotechnical Journal*, vol. 41, n. 4, pp. 686–697.
[12] Goodman, R. E., 1995. Block theory and its application. *Géotechnique*, vol. 45, n. 3, pp. 383–423.
[13] Cundall, P. A., 1988. Formulation of a three-dimensional distinct element model - Part I. A scheme to detect and represent contacts in a system composed of many polyhedral blocks. *International Journal of Rock Mechanics and Mining Sciences and Geomechanics Abstracts*, vol. 25, n. 3, pp. 107–116.
[14] Zaoui, A., 2002. Continuum micromechanics: Survey. *Journal of Engineering Mechanics*, vol. 128, n. 8, pp. 808–816.
[15] Hoek, E. & Brown, E. T., 1980. Empirical strength criterion for rock masses.
[16] Maghous, S., Dormieux, L., Kondo, D., & Shao, J. F., 2013. Micromechanics approach to poroelastic behavior of a jointed rock. *International Journal for Numerical and Analytical Methods in Geomechanics*, vol. 37, n. 2, pp. 111–129.
[17] Booker, J. R. & Randolph, M. F., 1984. Consolidation of a Cross-Anisotropic Soil Medium. *The Quarterly Journal of Mechanics and Applied Mathematics*, vol. 37, n. 3, pp. 479–495.
[18] Ai, Z. Y. & Wu, C., 2009. Plane strain consolidation of soil layer with anisotropic permeability. *Applied Mathematics and Mechanics (English Edition)*, vol. 30, n. 11, pp. 1437–1444.
[19] Rani, S., Kumar, R., & Singh, S. J., 2011. Consolidation of an Anisotropic Compressible Poroelastic Clay Layer by Axisymmetric Surface Loads. *International Journal of Geomechanics*, vol. 11, n. 1, pp. 65–71.
[20] Sasaki, T. & Morikawa, S., 1996. Thermo-mechanical consolidation coupling analysis on jointed rock mass by the finite element method. *Engineering Computations*, vol. 13, n. 7, pp. 70–86.
[21] Goodman, R. E., 1989. *Introduction to Rock Mechanics*. Wiley and Sons, 2 edition.
[22] Borges, A. B. & Maghous, S., 2020. Micromechanics Approach to the Effective Permeability of a Jointed Rock. In *XLI CILAMCE Proceedings*, pp. 7, Foz do Iguaçu (Online Edition, during COVID-19 Pandemic).
[23] Coussy, O., 2004. *Poromechanics*. Wiley.
[24] Brüch, A. R., 2016. *Simulação Numérica Tridimensional de Processos de Deformação em Bacias Sedimentares*. Tese de doutorado, Universidade Federal do Rio Grande do Sul.
[25] Bernaud, D., Deudé, V., Dormieux, L., Maghous, S., & Schmitt, D. P., 2002. Evolution of elastic properties in finite poroplasticity and finite element analysis. *Int. J. for Num. & Analyt. Methods in Geomech.*, vol. 26, n. 9, pp. 845–871.